

Estimation of Charge, Energy and Polarity of Noisy Partial Discharge Pulses

Rodrigo Mor, A.; Castro Heredia, Luis; Muñoz, Fabio

DOI

[10.1109/TDEI.2017.006381](https://doi.org/10.1109/TDEI.2017.006381)

Publication date

2017

Document Version

Final published version

Published in

IEEE Transactions on Dielectrics and Electrical Insulation

Citation (APA)

Rodrigo Mor, A., Castro Heredia, L., & Muñoz, F. (2017). Estimation of Charge, Energy and Polarity of Noisy Partial Discharge Pulses. *IEEE Transactions on Dielectrics and Electrical Insulation*, 24(4), 2511-2521. <https://doi.org/10.1109/TDEI.2017.006381>

Important note

To cite this publication, please use the final published version (if applicable). Please check the document version above.

Copyright

Other than for strictly personal use, it is not permitted to download, forward or distribute the text or part of it, without the consent of the author(s) and/or copyright holder(s), unless the work is under an open content license such as Creative Commons.

Takedown policy

Please contact us and provide details if you believe this document breaches copyrights. We will remove access to the work immediately and investigate your claim.

Estimation of Charge, Energy and Polarity of Noisy Partial Discharge Pulses

A. Rodrigo Mor, L. C. Castro Heredia

Delft University of Technology
Electrical Sustainable Energy Department
Delft, the Netherlands

and F. A. Muñoz

Universidad del Valle
Escuela de Ingeniería Eléctrica y Electrónica
Cali, Colombia

ABSTRACT

The algorithms for the computation of charge, energy and polarity of partial discharge (PD) pulses are affected by noise, which can lead to over and underestimation of the PD quantities. These quantities can be computed in time domain, frequency domain and according to the impulse response method (standard IEC270). In this paper, a theoretical study is performed in which each computation method is applied to simulated PD pulses having different waveforms and noise level to evaluate the extent of affectation on the results due to the noise. The results suggest that the error in the estimation of the PD charge is higher for oscillatory pulses regardless of the method. In contrast, the estimation of energy is more resilient to the PD waveform and the estimation in frequency domain gives rise to low error. In time domain, the charge and energy estimation method can be improved by filtering the PD pulse and integrating the output pulse to certain limits. A new method for the estimation of PD polarity is proposed based on the derivative of the filtered pulse, showing accurate estimation of the polarity even for the pulses with low signal to noise ratio.

Index Terms — Partial discharge, charge, energy, quasi-integration, pulse filtering.

1 INTRODUCTION

THE importance of partial discharge (PD) measurements for the diagnosis of high voltage equipment has motivated the development of a wide range of measuring circuits and instruments. Since the rise time of a PD pulse can typically be as short as a few nanoseconds then an important feature of a measuring instrument is its bandwidth. This is because it is closely related to the waveform of the recorded pulses. If an *ideal* measurement is achieved, the measured PD pulse should be unipolar with no oscillation. However, apart from the bandwidth, other factors affect the shape of the signals arriving to the sensors: the characteristics of the PD pulse at its origin, location of the PD source within the HV equipment and the distance of the PD source to the sensor. The location and distance of the PD source is relevant for the measurements because largely capacitive or inductive test objects such as stator windings, cables or gas insulated systems behave like transmission lines which yield to attenuation, distortion and oscillation of the recorded pulses [1, 2]. In practice, the pulse

signals are in addition distorted by the always present noise. The signals, are then processed by both time and frequency methods to estimate relevant parameters such as the apparent charge, energy and polarity. To accomplish this estimation accurately, the PD signals must often be extracted from noise, which is a challenging task due to the broad variety of noise sources. G. Stone makes a classification of noise sources as external and internal noise [3]. The external noise, e.g. arcing pulses, thyristor switching pulses, radio transmissions and PD pulses from the power system, can be thought as unwanted signals that may be erroneously processed as PD signals from the test object or swamp the PD signal of interest. The knowledge about the signal source has led to noise rejection techniques based on attributes of the PD signal and the noise, for instance, phase position, frequency spectrum (of the PD pulse and the noise), polarity, repetition rate and physical location, etc. The internal noise (also referred to as thermal noise or white noise) refers to the noise produced by thermally induced current fluctuations in the electronics of the measuring circuit. Often, the internal noise is seen as less harmful than the external one. Yet, the recent increase of popularity and availability of unconventional PD measuring systems can arise new concerns about the white noise added

due to the digitalization of the signals by the analogue-digital converter (ADC). As pointed in [4], an uniform step quantization would not represent adequately an analogue signal with a non-uniform amplitude distribution, as it is the case with many PD sources.

In addition, since no recommendations are given by any standard for the acquisition of PD signal by means of unconventional systems, then the relevant parameters for the acquisition such as the sampling frequency, the acquisition time, the number of samples, etc., are arbitrarily set. Results in [5] have shown that the computation of PD parameters from digital PD signals are indeed affected by the acquisition parameters which also might hinder the comparison between tests.

Both external and internal noise sources end up worsening the signal to noise ratio (SNR) of the signals. Ultimately, low levels of SNR can overcome the processing capabilities of the measuring systems. Bearing in mind the strong influence of the bandwidth on the waveform and the unavoidable presence of noise in the recorded signals, it is the aim of this paper to evaluate the performance of time and frequency domain methods in the estimation of charge, energy and PD pulse polarity when the PD current pulses have different SNR levels and as well as when they have different waveforms.

2 OVERVIEW OF THE EFFECT OF NOISE ON THE ESTIMATION OF PD PARAMETERS

By definition the electric charge Q of a PD current pulse $i(t)$ is the integral of the current in time according to the equation (1). In relation to a measuring system, the signal $i(t)$ is the actual PD current resulting after scaling the sensor output by its transfer function, being t_{pd} the pulse duration.

$$Q = \int_0^{\infty} i(t) dt = \int_0^{t_{pd}} i(t) dt \quad (1)$$

As can be seen, the former analytical definition requires the integration of the current pulse up to infinity. However, the value of charge is determined only by the area of the pulse. When $i(t)$ is a measured signal then the measuring process itself and the electromagnetic background, among other factors, will add noise and disturbances to the acquisition. Therefore the measured PD current signal $i_{meas}(t)$ becomes the equation (2) and the charge computation now has to take into consideration the sources of noise $n(t)$ as in the equation (3).

$$i_{meas}(t) = i(t) + n(t) \quad (2)$$

$$Q = \int_0^{\infty} i_{meas}(t) dt = \int_0^{\infty} i(t) dt + \int_0^{\infty} n(t) dt \quad (3)$$

The term $n(t)$ in the present contribution is defined as a Gaussian White Noise (GWN) component, which is typical from ADC noise. A remarkable feature of GWN is that it is a stationary random process with theoretically zero mean, having the property that any two values of GWN are statistically independent no matter how close they are in time [6]. Given this property of GWN, the evaluation of the

equation (3) should equal the equation (1) because the integral of $n(t)$ is zero when evaluated from zero to infinity.

When the signal is no longer continuous but discrete as digital PD signals, the result from the equation (3) differs from equation (1) because in discrete time, where a finite number of samples N are used to represent a signal having a sampling period $T=1/F_s$ (F_s sampling frequency) the mean value of the noise vector might not be zero. When dealing with discrete signals, then the equation (3) becomes the equation (4).

$$Q = T \cdot \sum_{k=1}^N i_{meas}(k) = T \cdot \left[\sum_{k=1}^N i(k) + \sum_{k=1}^N n(k) \right] \quad (4)$$

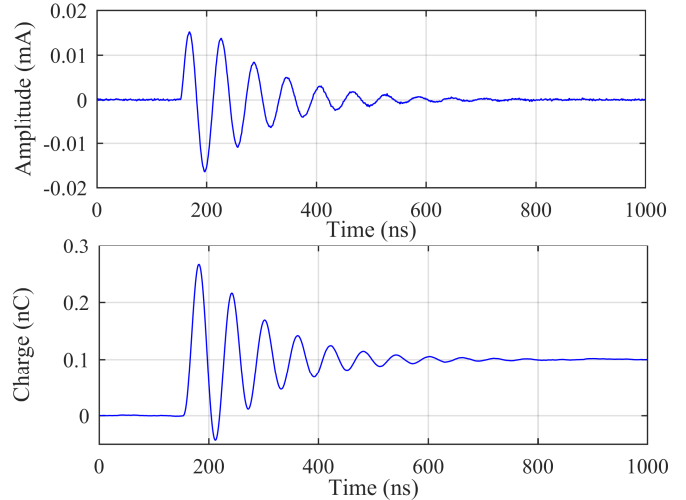


Figure 1. Oscillatory current pulse without noise (top). Cumulative integral of the current pulse to estimate the charge (bottom).

To illustrate the effect of white noise on the result of the equation (4), the charge of an oscillating PD current pulse without and with a certain level of noise is computed as shown in Figure 1 and Figure 2. The amplitude and period of the pulse were set to result in a charge of 100 pC.

As can be seen in Figure 1 the result of the charge value for the pulse without noise do not deviate from the expected value of 100 pC. For the case of the pulse having a level of noise (Figure 2) the computed value the computed value is roughly twice the expected value. In a general basis, the result can be either an underestimation or an overestimation depending on the particular characteristics of the noise. In addition, it seems plausible to claim that the acquisition parameters indeed affect the computation methods because the sampling rate, the number of samples, the vertical resolution, among other parameters related to the acquisition influence the level of signal to noise ratio.

Since a level of white noise is always present in practical measurements, alternative computation methods are required to counterbalance its influence. The computation of other significant parameters such as the pulse energy requires the evaluation of cumulative integrals thus being also affected by the noise. In the next sections, a detailed analysis will be presented of the performance of time and frequency domain methods and the impulse response method to compute charge, energy and pulse polarity when applied to signals resembling PD current pulses to which white noise was added.

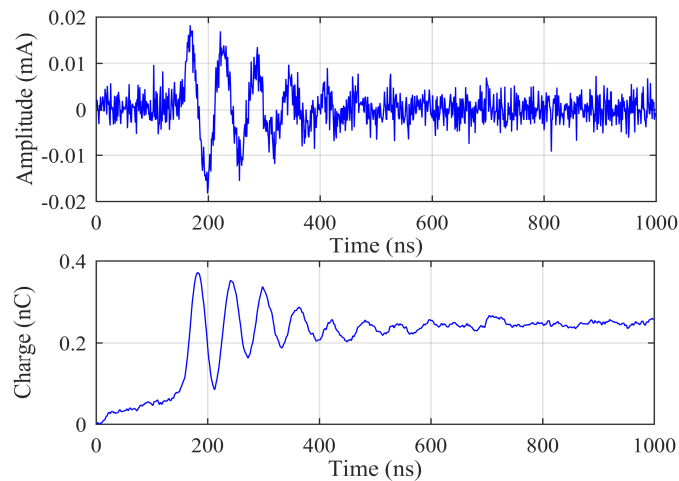


Figure 2. Oscillatory current pulse having a certain level of noise (top). Cumulative integral of the current pulse to estimate the charge (bottom).

3 PULSE WAVEFORMS

Different PD current pulses were generated by means of a math software having each a different waveform. A series of 5000 pulses were generated for each type of pulse. The pulse length was 1000 ns and the sampling frequency was 1 GS/s (time resolution 1 ns). The analytical equations used to generate every type of pulse are summarized in Table 1, whereas the shape of the generated pulses can be seen in Figure 3. To reconstruct such pulses, the units for the time t shall be ns and $u(t)$ is the step function. It can be noted as well that the pulses are shifted $t_0 = 150$ ns in time. The amplitude and coefficients in the analytical equations for each current pulse were chosen to result in a charge of 100 pC.

Table 1. Analytical Equations to Generate Each Type of PD Current Pulse.

TYPE	EQUATION
1	$p_1 = 1 \times 10^{-3} \cdot u(t-t_0) \cdot u(t_0+t_p-t); \quad t_p = 100 \text{ ns};$
2	$p_2 = 1.2649 \times 10^{-3} (t-t_0)^{0.5} \cdot e^{-0.05(t-t_0)} \cdot u(t-t_0);$
3	$p_3 = 5.6437 \times 10^{-5} (t-t_0)^{10} \cdot e^{-2(t-t_0)} \cdot u(t-t_0);$
4	$k_1 = (t-t_0)^{10} \cdot e^{-79.4328(t-t_0)^{0.1}} \cdot u(t-t_0);$ $p_4 = -1.00785 \times 10^{32} \cdot k_1 \cdot \cos(2\pi/100 \cdot t) \cdot e^{-t/400};$
5	$k_2 = (t-t_0) \cdot e^{-0.5228(t-t_0)^{0.4}} \cdot u(t-t_0);$ $p_5 = 0.004981 \cdot k_2 \cdot \sin(2\pi/60 \cdot t - t_0) \cdot e^{-(t-t_0)/200};$

From practical measurements it is well known that the pulse shapes at the recording point can vary from unipolar pulses to oscillatory pulses. As reported in [7], corona discharge pulses are examples of unipolar pulses with a pulse duration of the order of 100 ns for which pulses of type 1 and 2 are good representations. Other PD sources like free-moving particle discharges and internal discharges showed oscillatory behaviour as that described by pulses of type 4 and 5. In addition, Figure 3 allows to highlight that on account of pulse duration and oscillations the frequency spectrum of pulses may be very different than the theoretical flat spectrum usually assumed for PD pulses in literature. In this sense, the type of pulse 3 with a short duration of just 10 ns approaches the best to a flat spectrum.

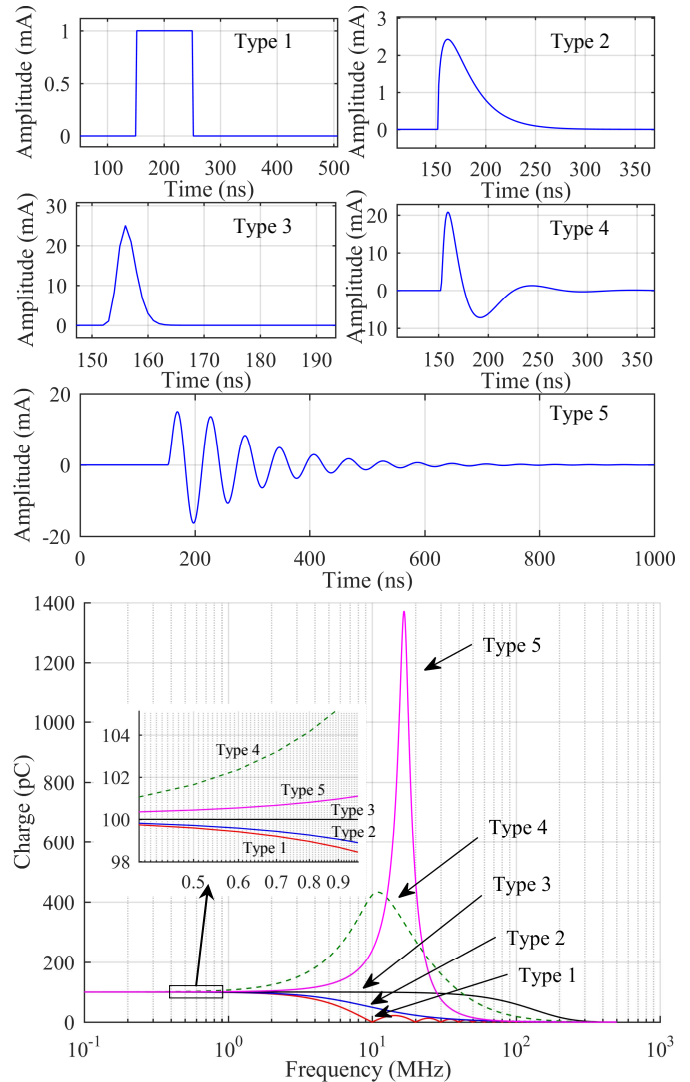


Figure 3. Waveforms corresponding to each pulse type and comparison of the corresponding frequency spectrum.

4 CHARGE ESTIMATION METHODS

The apparent charge of a PD pulse can be estimated by several methods both in time and frequency domain. In time domain, the charge value results from the time integral over the PD current pulse. In frequency domain, the low frequency components of the PD current pulse are used to approximate the charge value. The method proposed by the standard IEC270 is a particular impulse response method that requires the computation of a scale factor after a calibration with a pulse of known charge. The particularities for each method are described as follows.

4.1 FREQUENCY DOMAIN CHARGE ESTIMATION METHOD

The Fourier Transform of an ideal fast and very short current pulse results in a frequency spectrum being flat in a wide range of frequencies [8] as depicted in Figure 4. Furthermore, it can be claimed that the mean component (DC component) carries information about the area of the current pulse which is the charge value of the pulse.

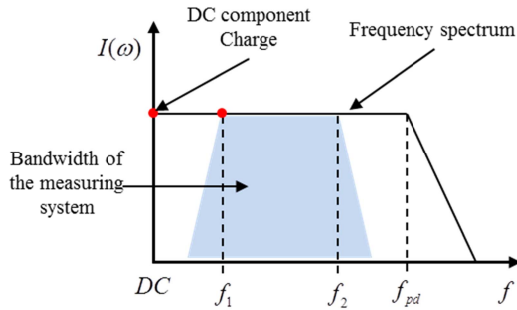


Figure 4. Theoretical frequency spectrum of a fast pulse showing a flat region until the frequency f_{pd} and the DC component which is related to the pulse charge.

Following the definition of the Fourier Transform $F(\omega)$ in the equation (5), it can be seen that for the mean component, $\omega=0$, the complex factor becomes the unity and the equation (5) equals the equation (1), so resulting in the value of charge.

$$F(\omega) = \int_{-\infty}^{\infty} f(t) \cdot e^{-j\omega t} dt \quad (5)$$

In practical measurements, the mean component is not measured by the PD sensor either because of the lower cut-off frequency of the sensor or because the DC component cannot induce a voltage in an inductive sensor such as a HFCT. However, the flat frequency spectrum provides the advantage that the amplitude of lower frequencies should equal the amplitude of the mean component. Therefore, the amplitude of the component f_i as measured by PD sensors should be still a good approximation to the amplitude of the DC component.

However, one limitation of this approach is that the accuracy of the approximation depends strongly on the pulse duration d . Let's consider a pulse shape of type 1 $f(t)$ having an amplitude k and duration d in the range of nanoseconds. Analytically, its Fourier Transform is that shown in equation (6).

$$F(\omega) = k \cdot d \cdot \frac{\sin(\pi \cdot d \cdot f)}{\pi \cdot d \cdot f} \quad (6)$$

When evaluating equation (6) for different values of d ; 1, 10, 100 and 1000 ns, the resulting frequency spectrum is that of Figure 5. The amplitude k of the pulse for each value of d was scaled to result in a charge of 100 pC, i.e.

By observing the resulting frequency spectrum, it is easy to note that the longer the pulse duration, the lower the frequency range that approximates best the value of charge. With a duration of 1000 ns, only the frequencies up to 250 kHz approach the 90% of the charge value. However, when the pulse duration is 1 ns, the frequency range increased to 250 MHz. Therefore, if the PD pulse is short enough a better approximation of the charge can be achieved by using the amplitude of the low frequency components.

The flow chart in Figure 6 shows the computation method to estimate the pulse charge in frequency domain. The sampled signal y_k is the PD current pulse and S_k is its corresponding Fourier Transform. For measured signals, the frequency spectrum is not flat and therefore the low frequency component is determined as the maximum component S_{pk} in a range up to 10 MHz. Finally the value of S_{pk} is multiplied by the sampling period to compute the charge.

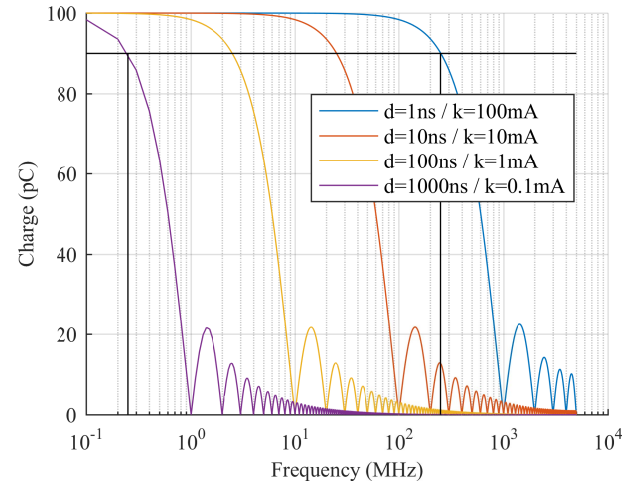


Figure 5. Frequency spectrum of a square pulse with varied duration d . The amplitude k of the pulse was scaled to result in a charge of 100 pC.

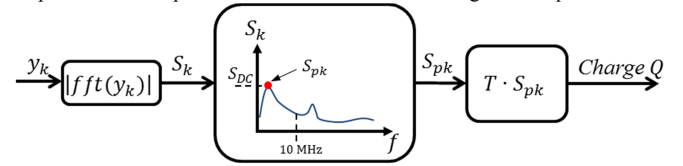


Figure 6. Flow chart for the computation of the charge in frequency domain.

4.2 IMPULSE RESPONSE CHARGE ESTIMATION METHOD

The charge estimation method proposed by the IEC270 is based on the impulse response of a band pass filter with specific bandwidth and cut-off frequencies.

Already in the early sixties, it was recognized that the apparent charge was the most meaningful quantity to be derived from PD measurements. As an attempt to standardize the measuring circuits and the procedures, the IEC Technical Committee No. 42 released the first version of the standard IEC270 in 1968 on the measurements of partial discharges expressed in terms of pC, which soon would become a widespread practice over the radio interference voltage (RIV), method that was available by then and introduced in America back in 1940 by NEMA publication 107. Up to the date, the standard IEC270 has been revised three times; in 1981, 2000 and 2015 [9]. The choice of the apparent charge was preferred since it has been shown that it correlates with the overall insulation degradation, it can provide indications about the size of insulation defects and along with the discharge inception voltage (DIV) it can be used to estimate the energy related to the discharge [10].

In compliance with IEC270, the time integration of the PD current pulses is approximated by analogue bandpass filtering. Some authors address that it would not be difficult to implement an electronic integrator to always compute accurate values of charge. However, they also claim that this might be problematic because of the frequency dependent gain of the integrator that would not achieve enough attenuation for the high frequencies and therefore radio interferences would not be rejected [11]. This problem and the search for avoiding additional electronic circuitry which can interact with the other components of the measuring and test circuit might have counterbalanced some of the drawbacks encountered with the analogue filtering method.

Resorting again to Figure 4, a bandpass filter having an upper cut-off frequency f_2 quite lower than the limiting frequency of the PD pulse f_{pd} will yield an output signal proportional to the product of the height of the flat spectrum of the PD pulse and the bandwidth of the filter, i.e. to the charge [11]. Since this filter is not achieving a true integration of the current pulse, this method is usually referred to as quasi-integration whose theoretical background and mathematical explanation can be found in [12, 13] thus shall not be discussed here. Because of the tight filtering, the time response output signal of the filter has a totally different shape and rather longer duration than the original PD pulse. The peak of this output, which is proportional to the charge, is readily detected by a peak detector. A calibration procedure is then needed to compute the factor scale that relates the magnitude of a known charge and the detected peak. Afterwards, the reading in mV is multiplied by the scale factor to calculate the charge value.

According to the standard IEC270 a conventional PD instrument for the measurement of charge is set provided the bandpass filter complies with certain limits for the bandwidth Δf and cut-off frequencies f_1 and f_2 . For the purposes of this paper, the values for wideband filtering are relevant. The lower cut-off frequency f_1 of the entire system is determined by the series connection of the coupling capacitor and the measuring impedance as depicted in the well-known conventional measuring circuits. Furthermore this frequency along with the roll-off of the bandpass filter suppress the high power frequency displacement currents including higher harmonics [14]. The upper frequency f_2 is closely related to the pulse resolution time; this is, the ability of the measuring system to resolve consecutive individual pulses without a significant increase of integration error, namely without pulse superposition. Thus, the wider the bandwidth the shorter the resolution time.

It is noteworthy that the recommendations only for the values of Δf , f_1 and f_2 were criticized soon after the first revision of the standard IEC270. Zaengl [13] pointed out that these parameters are just a part of the parameters that are required to establish the actual and complete transfer characteristics of the measuring system. The order and the type of the bandpass filter as well as the resolution time are also significant parameters to establish the transfer characteristics. He also claimed that universally comparable and unambiguous measurement results are only possible provided that the full transfer characteristic of the measuring system is known.

The calibration of the measuring system has been also the target of critical comments because it might go unnoticed that the duration and shape of the calibration pulse impact strongly on the ability of the measuring system to integrate a given PD current pulse properly or not. For an accurate pseudo-integration, the PD pulse has to be fast enough so that the requirement that f_{pd} be much higher than f_2 is met. In other words, if the pulse duration becomes longer, then the length of the flat part of the spectrum will be shorter and it might happen that the bandwidth of the filter covers an uneven part

of the pulse spectrum leading to integration error. This requirement applies also to the calibration pulse by which the scale factor is calculated. From the simulation results offered in [11], the sensitivity of a measuring system expressed as the ratio of peak amplitude of the filter output to the charge of the pulse at the filter input ($\mu\text{V}/\text{pC}$) can be claimed as dependant on the rise time of pulse and bandwidth of filter. A filter with a narrow bandwidth in the order of tens of kHz resulted in a low sensitivity but the pulse period can be longer without significant integration error. Conversely, a wider bandwidth in the range of 1-2 MHz has the effect of resulting in a high sensitivity only for very short pulses, but with increasing pulse period the error of integration increases fast. Similar simulation results showed that the parasitic inductance in the measuring circuit affects the calibration of the system according to the rise time and bandwidth of the filter, that if not considered may lead to erroneous measurement results [15].

So far it is clear that the IEC270-based method requires a calibration procedure that cannot be claimed as valid for any pulse waveform. In practice, numerous factors may distort the pulse waveforms or increase its period and hence it is likely that the quantification of charge values by different measuring instrument differs significantly.

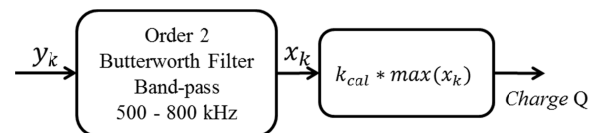


Figure 7. Flow chart for the computation of the charge in time domain according to impulse response method.

In order to compute the charge according to the impulse response method, a digital, second order Butterworth filter was used as depicted in the flow chart of Figure 7. The values of f_1 and f_2 for the filter were set to 500 kHz and 800 kHz respectively. These values were chosen after testing different cut-off frequencies for the filter as will be discussed in section 7.3. The sampled signal y_k is the PD current pulse and x_k is the output of the filter whose peak amplitude is multiplied times the scale factor k_{cal} to compute the charge. A unique value of k_{cal} was computed for the pulse type 3 and this scale factor was used to compute the charge for all of the types of pulses.

4.3 TIME DOMAIN CHARGE ESTIMATION METHOD WITH LOW-PASS FILTER

In time domain, provided the bandwidth of the measuring systems lies down in the range of tens of MHz, which is usually enough to resolve the pulse shape, the charge is estimated by the peak of the cumulative integral over the PD current pulse.

If the sampled signal y_k is of the type 2 or 3 according to Table 1, the result of the cumulative integration of the signal is an increasing curve that reaches its maximum at the end of the pulse duration and remains this value until the end of the acquisition time. Thus, the charge is determined by the maximum of the cumulative integral. For the case of oscillating pulses the computation of the charge has the problem that the cumulative integral of the signal is also oscillatory. In this case, the charge is

not at the maximum but at the steady-state value of the cumulative integral. For this oscillatory pulses, the value of the cumulative integral at the end of the acquisition cannot estimate correctly the values of charge because, as was illustrated in Figure 2, the noise level in the signal affect the value of the integral leading to error.

As a means to avoid the effect of the oscillation on the estimation of the charge, in this paper a method is proposed in which the original pulse is filtered by a low-pass, second order, Butterworth filter and then the cumulative integration is evaluated over the filtered pulse. The cut-off frequency of this filter is 2 MHz. The advantage of this approach is illustrated in Figure 8. The oscillatory pulse at top-left is filtered giving rise to the unipolar pulse at top-right. The cumulative integral over this unipolar signal results in a plot with a maximum corresponding to the charge value.

To eliminate the oscillations of the pulse by means of the low-pass filter brings about the further advantage that the limits of the output pulse (marked as black dots in Figure 8) can be readily approximated. When the cumulative integral of the pulse is evaluated only over these limits, the effect of noise and disturbances in the sample signal on the integral can be mitigated.

The flow chart in Figure 9 shows that after filtering, the indexes of zero-crossing points of the first peak of the output signal x_k need to be computed. These indexes define the limits for the cumulative integral.

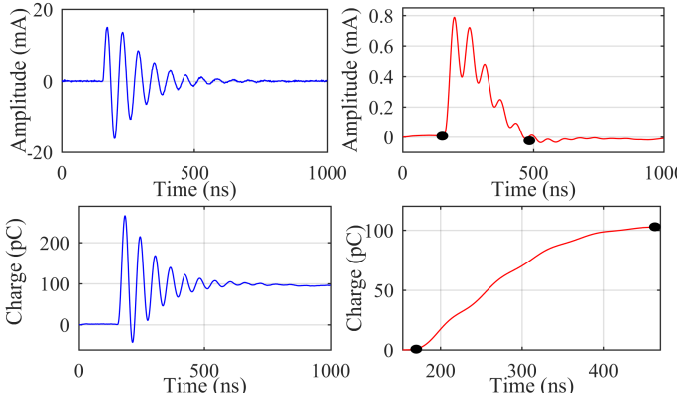


Figure 8. Low-pass filtering of oscillatory pulses for the estimation of charge in time domain. Oscillatory PD pulse (top-left), Filtered pulse (top-right), Cumulative integral of the oscillatory PD pulse (bottom-left), Cumulative integral of the filtered pulse (bottom-right).

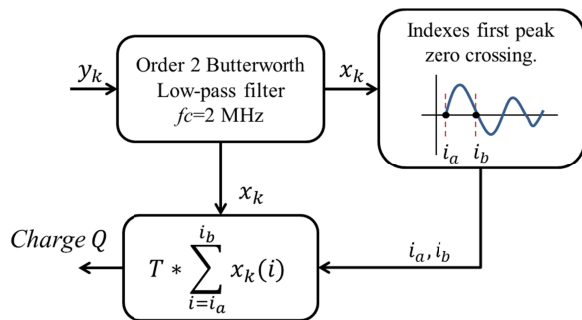


Figure 9. Flow chart for the computation of the charge in time domain.

5 ENERGY ESTIMATION METHODS

In unconventional PD measuring systems, the PD signal is acquired as a voltage signal terminated at the impedance of the

digitizer R , usually 50Ω . If the PD voltage signal is v_k , then the power of the signal P_k is defined as in the equation (8) and the energy E_k as in the equation (9), being N the number of samples.

$$P_k = \frac{(v_k)^2}{R} \quad (8)$$

$$E_k = \frac{T}{R} * \sum_{i=i_a}^{i_b} (v_k(i))^2 = \frac{T}{R \cdot N} * \sum_{i=f_a}^{f_b} |fft(v_k)|^2 \quad (9)$$

The equality in the equation (9) refers to the Parseval's theorem, stating that the energy of a signal can be computed both from time and frequency domain.

The algorithms already described for the estimation of charge can be applied almost identically for the computation of energy, except that the input signal has to be replaced by P_k . Only in frequency domain the algorithm had subtle changes as requested by the equation (9). The flow charts in Figure 10 show the energy computation methods based on time and frequency domains as were implemented for the simulation in this paper.

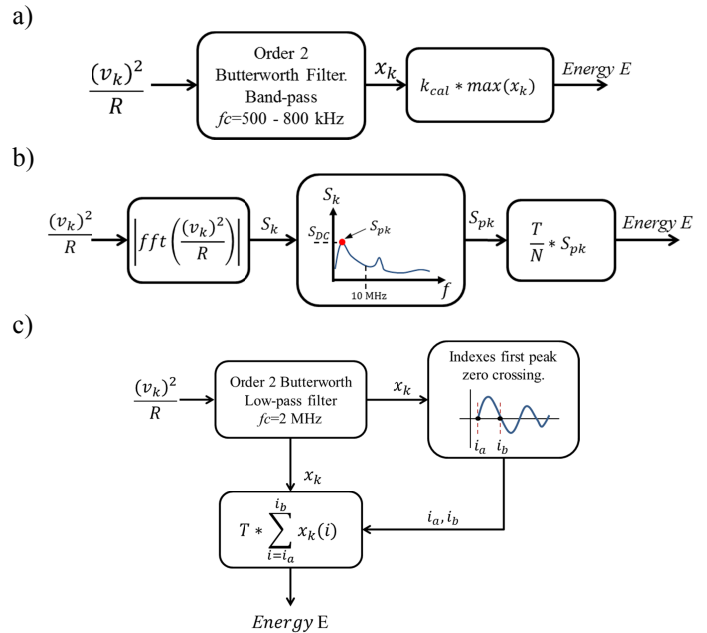


Figure 10. Flow chart for the computation of the PD pulse energy: a) impulse response method, b) in frequency domain and c) in time domain.

6 PULSE POLARITY CALCULATION METHOD

The polarity of the PD pulses cannot always be directly determined from the sign of the first peak of the original pulse. Both the noise and the oscillations could modify the peak value, leading to a wrong computation of the pulse polarity. This case is observed in Figure 11a where a positive oscillatory pulse happened to have a negative maximum peak. In addition, it can be seen that the maximum not necessarily occurs at the first peak of the pulse. When filter-based method as that of the standard IEC270 are implemented, the noise can distort the output of the filter such that it is not feasible to compute the

polarity from the sign of the peak of the filtered pulse. From Figure 11b that corresponds to the IEC270-filtered output signal of the positive pulse in Figure 11a, it is not obvious that the input pulse has positive polarity, and in fact the first peak has negative polarity.

As an approach to compute the polarity of pulses that is more resilient to oscillation and noise, in this paper a derivative method of the filtered output signal has been implemented. First, the input pulses are fed into a second order, Butterworth filter with a lower cut-off frequency of 10 kHz and upper frequency of 500 kHz. Then, the approximate discrete derivative of the output signal is computed (Figure 11c). If the assumption is made that the actual pulse should have the highest rise time than any other oscillation in the output signal, then the sign of maximum peak of derivative curve succeeds in computing the polarity of the input pulse.

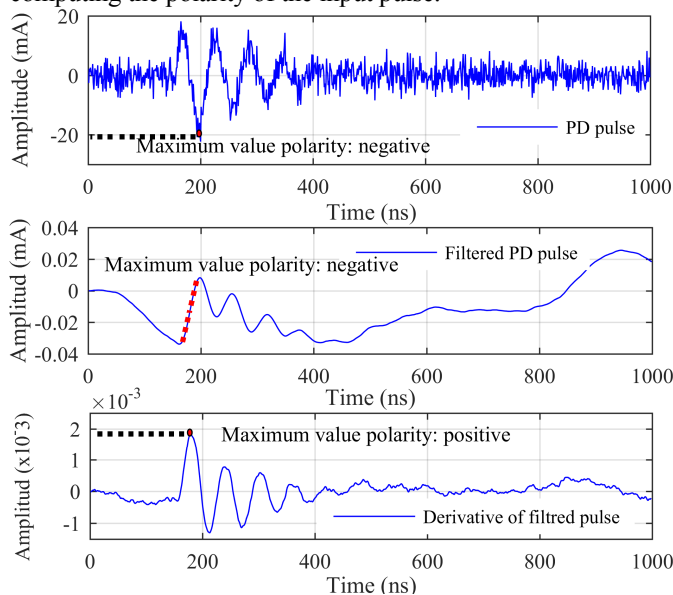


Figure 11. Filtering of PD pulse and derivative method for the computation of pulse polarity: top) input PD signal, middle) filtered pulse and bottom) derivative of the filtered pulse.

7 CHARGE ESTIMATION RESULTS

The simulation study consisted of evaluating the effect of the Gaussian White Noise on each of the methods for charge and energy estimation. For this analysis, the pulses listed in Table 1 were scaled to 100pC and for the set of 5000 pulses of each type the signal to noise ratio (SNR) was varied from 1dB to 30dB. The reference values of energy were computed as well for each pulse type (without noise) and are summarized in Table 2.

For each pulse type, the effect of noise was evaluated through the statistical parameters σ and $\Delta\mu$. The reference values were computed by means of the time integrals over the original pulses without noise listed in Table 1. The values of $\Delta\mu$ refer to the variation of the computed value over the pulse with a SNR of 30dB with respect to the reference value. With a SNR of 30dB the noise level is almost negligible, therefore the values of $\Delta\mu$ are accounting only for the variation of each computation method when compared to the result of evaluating the time integrals in the definition of charge and

energy. The values of σ represent the standard deviation of errors of the 5000 pulses having different SNR levels.

Table 2. Reference Values of Charge and Energy for Each Pulse Type.

Type	CHARGE [pC]	ENERGY [pJ]
Type 1	100	0.1000
Type 2	100	0.1598
Type 3	100	1.7620
Type 4	100	5.5836
Type 5	100	14.109

Due to space limitations, only the results of charge values as a function of SNR for the pulse type 5 will be discussed in detail in the next sections. The results corresponding to the other pulse types will be discussed by means of the values of $\Delta\mu$ and σ .

7.1 RESULTS OF CHARGE ESTIMATION METHOD IN TIME DOMAIN

The charge values computed in time domain for the pulse type 5 are presented in Figure 12, where can be observed that the scatter of the results increased as the SNR decreased.

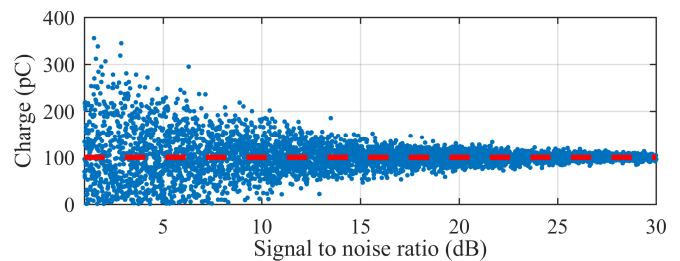


Figure 12. Results of the charge estimation method in time domain for the oscillatory pulse type 5.

At lower SNR, it was possible to see a significant effect of noise over the computation of the charge. For instance, in some cases the charge value was overestimated, reaching values as high as 350 pC, i.e. 3.5 times higher than the reference value. There were other cases where a critical underestimation was also possible leading to charge values of 0 pC. For the pulse whose charge was overestimated to 350 pC, the filtered pulse shown in Figure 13 (top-right) still did not reach a steady value before the pulse length of 1000 ns, and therefore the cumulative integral Figure 13 (bottom) had an increasing trending without any obvious local maximum.

The examination of the pulses that deviated the most from the reference value and with the lowest SNR showed large DC components (0 Hz) in the frequency spectrum of the noise. As an example, the noise signal and its frequency spectrum, added to a pulse resulting in a SNR of 1.93dB is shown in Figure 14. For this pulse, the DC component of the noise is roughly 250 pC and the value of charge was overestimated to 347 pC, which means an error of 247%.

Contrasting with the previous case, Figure 15 depicts the noise signal and its frequency spectrum for a pulse that despite having SNR of 1.15dB, the DC component of the noise happened to be very low, 14 pC. Note that in Figure 14 and Figure 15 only frequencies up to 10 MHz are plotted. The higher frequencies are removed by the Butterworth filter so they do not affect the charge computation.

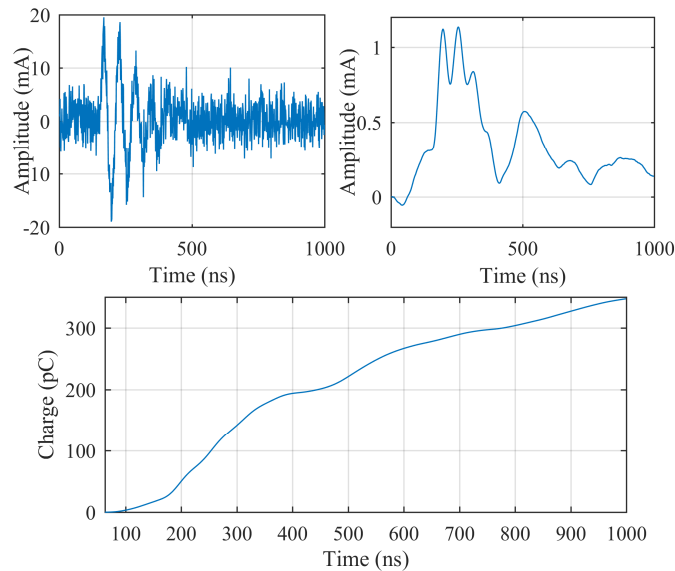


Figure 13. Pulse type 5 for which the charge value was overestimated to 350 pC. Pulse signal having a SNR of 1.93dB (top-left), Filtered pulse (top-right), cumulative integral of the filtered pulse (bottom).

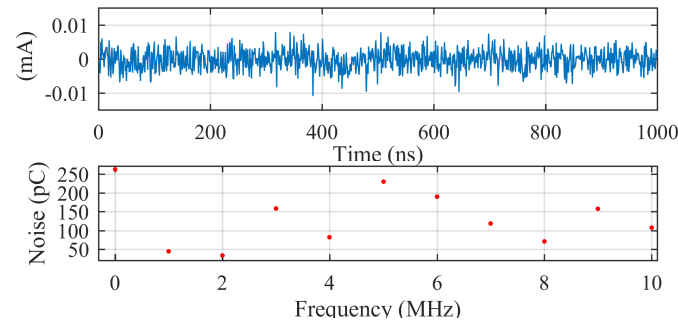


Figure 14. Noise signal and its frequency spectrum for a pulse with SNR of 1.93dB and estimated charge of 347 pC.

In general, it was observed that the estimation of charge deviated the most for those pulses whose added noise had large DC components at low frequencies. Because of its random behaviour, at low SNR the noise can lead to overestimation or underestimation of the charge value.

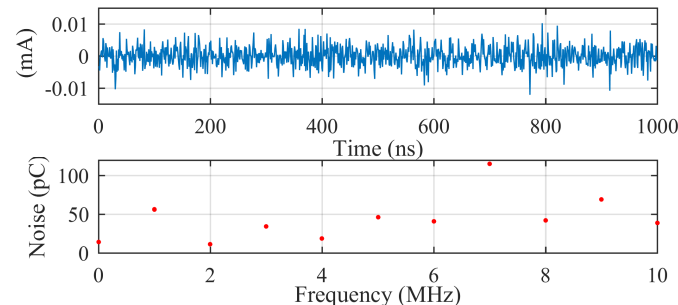


Figure 15. Noise signal and its frequency spectrum for a pulse with SNR of 1.15dB and estimated charge of 101 pC.

As the SNR increases the estimation of charge is less affected by the noise and the results tend to cluster around the reference value of charge as can be noted in Figure 12.

The statistical analysis through the variation of $\Delta\mu$ and σ for all pulse types is shown in Table 3. In addition, the charge values were computed without filtering the pulse signals, i.e. evaluating the cumulative integral over the original noisy pulses, in order to compare results from both methods.

Table 3. Statistical Analysis of the Charge Estimation in Time Domain with and without Filtering of Pulses.

Type	Filtered Time Domain		Time Domain	
	$\Delta\mu$ [%]	σ [%]	$\Delta\mu$ [%]	σ [%]
Type 1	4.1	2.2	-0.2	3.4
Type 2	3.9	2.6	-0.6	4.4
Type 3	5.3	9.4	0.3	14.7
Type 4	8.4	25.4	2.0	25.2
Type 5	5.0	27.1	0.0	36.7

In general terms, the estimation method upon the filtered pulses provides accurate results of charge as supported by the lower values of σ , meaning less scatter of the results, compared to the time domain method without filtering. For example, the deviation for the set of charge values of the pulse type 5 had a reduction of almost 10%, decreasing from 36.7% to 27.1%. Nevertheless, the values of $\Delta\mu$ are slightly higher with this method.

7.2 RESULTS OF CHARGE ESTIMATION METHOD IN FREQUENCY DOMAIN

The results of the charge estimation for the pulse type 5 as a function of SNR are shown in Figure 16.

The estimation of charge in frequency domain turned out being affected in the same way as with the method in time domain, i.e. the scatter of results increased with decreased SNR. However, the method in frequency domain appear to be more accurate compared to the results in time domain, hence the values of $\Delta\mu$ are lower as can be noticed after comparing Table 3 and Table 4.

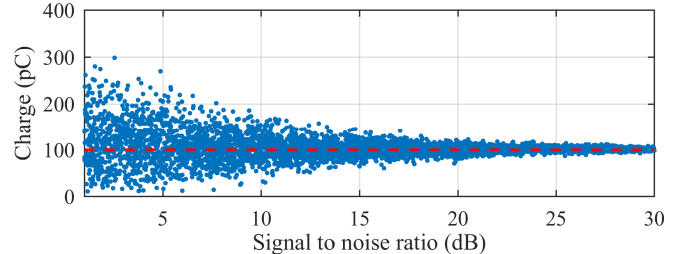


Figure 16. Results of the charge estimation method in frequency domain for the oscillatory pulse type 5.

Table 4. Statistical Analysis of the Charge Estimation in Frequency Domain.

Type	$\Delta\mu$ [%]	σ [%]
Type 1	-1.7	2.4
Type 2	-1.0	3.1
Type 3	-0.2	7.0
Type 4	6.5	18.3
Type 5	0.0	27.0

The deviation of errors σ resulting in frequency domain slightly decreased, particularly for the pulse type 4 and 3. The estimation of the charge for the pulse types 1 and 2 showed the lowest dispersion, as opposed to the oscillatory pulse type 5 whose error deviation was the highest regardless the computation method.

7.3 RESULTS OF IMPULSE RESPONSE CHARGE ESTIMATION METHOD

Of particular interest for this paper was to vary the relationship between the pulse frequency spectrum and

filter bandwidth and limiting frequencies, considering frequencies within and beyond those recommended in the standard IEC270. The specific values for each case of study are summarized in Table 5 as well as the statistical analysis of the results of the charge estimation. In this first sensitivity analysis, only the pulse type 5 were used to test each filter due to its oscillatory waveform.

Table 5 highlights that the deviation σ in the charge estimation values decreases as the cut-off frequencies of the filters increased. For instance, for the filter with cut-off frequencies of 100-200 kHz the deviation value was 27.2%, but with cut-off frequencies of 800-900 kHz the deviation value was reduced down to 17%. This reduction of the deviation can be observed in Figure 17 where clearly is noticed that the estimated charge values remain more clustered around the reference value of 100 pC.

Table 5. Performance Analysis of Filters according to Impulse Response method and Statistical Analysis of Charge Estimation for Pulse Type 5.

#	Bandwidth [kHz]	f_1 [kHz]	f_2 [kHz]	$\Delta\mu$ [%]	σ [%]
1	90	10	100	1	27.3
2*	100	100	200	1.3	27.2
3	100	400	500	-0.1	19.5
4	100	600	700	0.7	18.8
5	100	700	800	-0.1	17.1
6	100	800	900	1.2	17
7	190	10	200	0.3	28.3
8*	200	100	300	-0.5	27.2
9	200	500	700	1.6	18.2
10	200	600	800	2.0	17.5
11	200	700	900	-1.7	16.1
12	290	10	300	9.4	27.5
13*	300	100	400	-2.3	22.6
14	300	400	700	1.3	18
15	300	500	800	2.5	17.8
16	300	600	900	0.1	16.9
17	400	10	400	1.0	25.5
18	400	300	700	-2.3	18.3
19	400	400	800	1.8	18
20	400	500	900	-2.3	16
21	500	10	500	-2.9	23.7
22	500	300	800	0.9	18.2
23	500	400	900	-3.9	17.1

*filters within IEC270 limits

To increase the cut-off frequencies might result in a way to filter out the low-frequency components of noise, especially the DC component that, as was discussed in previous section, can have large magnitudes affecting the charge estimation.

In addition, the upper cut-off frequency seemed to have a larger effect on the reduction of the deviation than the increase of the bandwidth. Consistently, all filters with upper cut-off frequency of 900 kHz showed the lowest values of deviation regardless the bandwidth of the filter. Conversely, the filters with the lowest lower cut-off frequency led to the highest deviation of the results, with just a slight reduction for the cases of filters with bandwidth of 400 and 500 kHz.

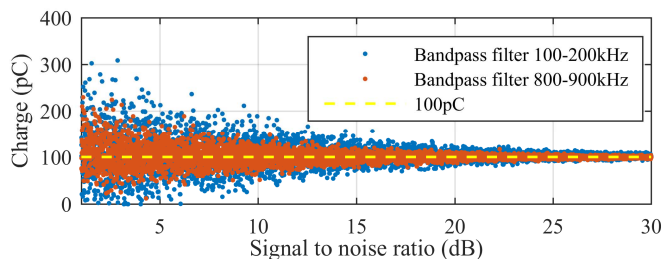


Figure 17. Effect of the increase of the bandpass filter cut-off frequencies on the dispersion of the charge estimation values.

As suggested by low values of $\Delta\mu$, the computed values of charge remained around 100 pC almost regardless of the tested filter. The highest variation of $\Delta\mu$ of 9.4% was for the case of the filter with bandwidth of 290 kHz, without any obvious correlation to the parameters of the filter.

The second analysis that was conducted was to apply the filters that gave rise to the lowest deviation, i.e. those with $\sigma < 18\%$, to all of the pulse types considered in this paper. In practical measurements, an IEC measuring system is calibrated with a pulse waveform that can be very distinct from the waveforms of the PD pulses reaching the bandpass filter. Due to this, the calibration factor for each filter was computed by using only the waveform of the pulse type 3. The results of this analysis are presented in Table 6.

Table 6. Statistical Analysis for Filters 5, 6, 10, 11, 14, 15, 16, 19, 20 and 23.

Type	Filter # 5		Filter # 6		Filter # 10		Filter # 11	
	$\Delta\mu$ [%]	σ [%]						
Type 1	-1.8	1.6	-3.7	1.5	-2.6	1.5	-3.0	1.5
Type 2	-1.6	2.0	-2.7	1.9	-2.0	1.9	-2.4	1.9
Type 3	1.1	6.3	-0.8	6.7	-0.6	6.7	-0.6	6.8
Type 4	9.8	11.7	9.1	10.2	8.5	11.5	10.1	11.5
Type 5	5.4	17.1	9.2	17.4	4.7	17.6	6.7	16.7

Type	Filter # 14		Filter # 15		Filter # 16		Filter # 19	
	$\Delta\mu$ [%]	σ [%]						
Type 1	-1.6	1.8	-1.6	1.7	-2.0	1.5	-1.7	1.7
Type 2	-1.0	2.2	-1.0	2.1	-1.1	1.9	-1.3	2.2
Type 3	0.2	7.5	-0.4	6.7	0.5	6.4	-0.1	7.4
Type 4	8.0	12	7.5	11.3	12.5	11.3	8.1	12.1
Type 5	2.0	18.8	2.8	17.9	6.7	16.5	6.1	18.5

Type	Filter # 20		Filter # 23	
	$\Delta\mu$ [%]	σ [%]	$\Delta\mu$ [%]	σ [%]
Type 1	-3.0	1.6	-0.8	1.5
Type 2	-2.3	1.9	-0.4	2.0
Type 3	-0.7	6.8	0.5	6.8
Type 4	9.1	11.0	10.4	11.4
Type 5	5.0	18.4	6.8	18.6

The collection of the results for the several filters tested allowed to be aware in a straightforward way of the error in the charge estimation that is achieved on account of a calibration factor computed from a particular waveform. Pulse type 1 and 2 are non-oscillatory with a waveform similar to that of type 3 (used as calibration pulse) and therefore it is reasonable to ascribe their low values of $\Delta\mu$ to the similarities of the waveforms. As the pulse waveform starts to differ from the calibration pulse, as in the case of the oscillatory pulse type 4 and 5, the error in the charge estimation increased with

a factor of at least few times. As can be seen in the zoom in the frequency spectrum of Figure 3, the resonance peak around 10 MHz for the pulse type 4 results in frequency components larger than those for the pulse type 3 within the frequency range of the filters. This explains also why the values of $\Delta\mu$ for the pulse type 4 were always higher for all the filters.

Regarding the effect of noise on the charge estimation, the deviation showed for all the cases of study an increase from the non-oscillatory pulses to the oscillatory ones regardless of the filter tested. It is also interesting to note that the filter #15 with frequencies of 500-800 kHz led to the lowest values of $\Delta\mu$. On the other hand, the change in the cut-off frequencies did not show a significant reduction of the deviation σ . This is, the values of deviation for each pulse type remained almost unchanged, e.g. for the pulse type 1, σ was around 1.5% and for the pulse type 5, σ was around 18% regardless of the filter frequencies.

8 ENERGY ESTIMATION RESULTS

In the estimation of the energy, when the time integral is evaluated directly over the pulses without any filter, the error increases with decreasing SNR. In fact, the effect of noise led to deviation values of 18% as can be noted in Table 7. By filtering the signals, a slight reduction of the error in the energy estimation is achieved and the deviation values decreased down to around 15%. In contrast, a significant reduction of the deviation is obtained by means of the methods in frequency domain and impulse response.

Table 7. Statistical Analysis of Energy Estimation.

Type	Time domain		Filtered time domain		Frequency domain		Impulse response	
	$\Delta\mu$ [%]	σ [%]	$\Delta\mu$ [%]	σ [%]	$\Delta\mu$ [%]	σ [%]	$\Delta\mu$ [%]	σ [%]
Type 1	-0.1	18.3	4.3	15	-1.5	2.2	-1.7	5.8
Type 2	0.1	18.4	4.0	14.9	-0.7	2.2	-0.3	5.6
Type 3	0.0	18.4	4.2	15.1	-0.2	2.5	0.1	5.7
Type 4	0.0	18.3	4.4	14.9	-0.4	2.2	-0.3	5.5
Type 5	0.1	18.2	2.6	15.6	-6.7	2.1	-7.2	5.9

By the impulse response method the deviation is around 5.5%, whereas the lowest deviation of roughly 2.2% was computed by the method in frequency domain. It is also noticeable that the computation of energy in frequency domain and by impulse response method gives rise to very low values of $\Delta\mu$ for pulse types 1, 2, 3 and 4. The square of the pulse in the energy computation has the effect of make larger the differences between the amplitudes of the pulse. Thus, the pulse might be assumed as having less noise level, which might explain the low values of $\Delta\mu$. On the other hand, for the pulse type 5 the values of $\Delta\mu$ were comparatively much higher than for the other pulse types.

9 ESTIMATION OF PULSE POLARITY

The method based on the derivative of the filtered output signal proved to accurately estimate the pulse polarity. After applying this method, the positive polarity of all of the pulse types was correctly estimated.

10 CONCLUSION

In digital measuring systems, the SNR affects the estimation of charge and energy to a different extent depending on the computation method. In general, the scatter of the results increased with decreased signal to noise ratio. The effect of the noise on the results was observed as a large under or overestimation of the computed values. This was the case for some of the oscillatory pulses of type 5, in which the charge value was overestimated in 250% with respect to the reference value of 100 pC. Underestimation of the charge value was also possible leading to a null value.

It was observed that the oscillatory pulses led to the highest scatter of the charge values due to the noise. For example, the deviation σ of the charge values computed in frequency domain for the pulse type 5 was 27%, whereas for those non-oscillatory pulses (type 2 and 3) the deviation was around 5%. In contrast, for the energy computation, the pulse waveform did not affect significantly on the deviation of the computed values.

Based on the results from Table 7, it can be claimed that the energy estimation method in frequency domain gives rise to the lowest error in the estimation.

The charge and energy estimation method in time domain was enhanced by filtering the signal and establishing specific integration limits, being this particularly suitable to overcome the negative effect of oscillation on the accuracy of the estimation. In estimating the charge, it was possible to reduce the deviation σ for the pulse type 5 from 36.7% to 27.1% after the filtering of the signal. It is also noticeable that the estimation of charge deviated the most for those pulses whose added noise had large DC components and large low frequency components.

In frequency domain, the deviation in the charge estimation was similar than that resulting from the time domain method, however lower values of $\Delta\mu$ were obtained in frequency domain.

Regarding the charge estimation by means of the impulse response method, it can be concluded that the deviation σ decreases as the cut-off frequencies of the filters increased. For instance, for the filter with cut-off frequencies of 100-200 kHz the deviation value was 27.2%, but with cut-off frequencies of 800-900 kHz the deviation value was reduced down to 17%.

In addition, the upper cut-off frequency seemed to have a larger effect on the reduction of the deviation than the increase of the bandwidth. Consistently, all filters with upper cut-off frequency of 900 kHz showed the lowest values of deviation regardless the bandwidth of the filter. Conversely, all of the filters with the lowest lower cut-off frequency led to the highest deviation of the results.

REFERENCES

- [1] IEC 60270-2000, "High-Voltage Test Techniques – Partial Discharge Measurements".
- [2] G. Stone, "Importance of bandwidth in PD measurement in operating motors and generators", IEEE Trans. Dielectr. Electr. Insul., Vol. 7, No. 1, pp. 6–11, 2000.

- [3] G. C. Stone, "Partial Discharge - Part VII: Practical Techniques for Measuring PD in Operating Equipment", IEEE Electr. Insul. Mag., Vol. 7, No. 4, pp. 9–19, 1991.
- [4] I. Shim, J. J. Soraghan, and W. H. Siew, "Digital Signal Processing Applied to the Detection of Partial Discharge: An Overview", Electr. Insul. Mag. IEEE, Vol. 16, No. 3, pp. 6–12, 2000.
- [5] A. R. Mor, L. C. Castro Heredia, and F. Muñoz, "Effect of Acquisition Parameters on Equivalent Time and Equivalent Bandwidth Algorithms for Partial Discharge Clustering", Int'l. J. Electr. Power Energy Syst., Vol. 88, pp. 141–149, 2017.
- [6] V. Z. Marmarelis, "Appendix II: Gaussian White Noise," in *Nonlinear Dynamic Modeling of Physiological Systems*, Wiley-IEEE Press, New Jersey p. 541, 2004.
- [7] A. Rodrigo Mor, L. C. Castro Heredia, and F. A. Muñoz, "New clustering techniques based on current peak value, charge and energy calculations for separation of partial discharge sources", IEEE Trans. Dielectr. Electr. Insul., Vol. 24, No. 1, pp. 340–348, 2017.
- [8] A. Cavallini, G. C. Montanari, and M. Tozzi, "PD apparent charge estimation and calibration: A critical review", IEEE Trans. Dielectr. Electr. Insul., Vol. 17, No. 1, pp. 198–205, 2010.
- [9] E. Lemke, "Guide for partial discharge measurements in compliance to IEC 60270", 2008.
- [10] L. Satish and W. S. Zaengl, "An effort to find near-optimal bandpass filter characteristics for use in partial discharge measurements", Europ. Trans. Electr. Power, Vol. 4, No. 6, pp. 557–563, 1994.
- [11] P. Osvath, E. Carminati, and A. Gandelli, "A Contribution on the traceability of partial discharge measurements", IEEE Trans. Electr. Insul., Vol. 27, No. 1, pp. 130–134, 1992.
- [12] A. R. Mor, P. H. F. Morshuis, and J. J. Smit, "Comparison of charge estimation methods in partial discharge cable measurements", IEEE Trans. Dielectr. Electr. Insul., Vol. 22, No. 2, pp. 657–664, 2015.
- [13] W. S. Zaengl, K. Lehmann, and M. Albiez, "Conventional pd measurement techniques used for complex HV apparatus", IEEE Trans. Electr. Insul., Vol. 27, No. 1, pp. 15–27, 1992.
- [14] E. Kuffel, W. S. Zaengl, and J. Kuffel, "Non-destructive insulation test techniques," in *high voltage engineering fundamentals*, 2nd ed., Newnes, Ed. Butterworth-Heinemann, pp. 395–455, 2000.
- [15] M. M. Twiel, B. G. Stewart and I. J. Kemp, "An investigation into the effects of parasitic circuit inductance on partial discharge detection," Electr. Insul. Conf. Electr. Manufacturing and Coil Winding Conf., Cincinnati, OH, pp. 213–217, 2001.



Armando Rodrigo Mor (M'14) is an Industrial Engineer from Universitat Politècnica de València, in Valencia, Spain, with a Ph.D. degree from this university in electrical engineering. During many years he has been working at the High Voltage Laboratory and Plasma Arc Laboratory of the Instituto de Tecnología Eléctrica in Valencia, Spain. Since 2013 he is an Assistant Professor in the Electrical Sustainable Energy Department at Delft University of Technology, in Delft, The Netherlands. His research interests include monitoring and diagnostic, sensors for high voltage applications, high voltage engineering, and HVDC.



Luis Carlos Castro was born in Cali, Colombia in 1986. He received the Bachelor and Ph.D. degrees in electrical engineering from Universidad del Valle, Cali, in 2009 and 2015 respectively. Currently, he is a post-doc in the Electrical Sustainable Energy Department at Delft University of Technology, in Delft, The Netherlands. His research interests include accelerated aging of stator insulation, monitoring and diagnostic tests.



Fabio Andrés Muñoz was born in Cali, Colombia, in 1988. He received the B.S. degree in electrical engineering from the Universidad del Valle, Cali, in 2011. He is currently a Ph.D. candidate in Electrical Engineering at Universidad del Valle. His main research interests are focused on high voltage engineering, insulation diagnostics and electrical machines.